

Growth and band alignment of Bi₂Se₃ topological insulator on H-terminated Si(111) van der Waals surface

Handong Li, Lei Gao, Hui Li, Gaoyun Wang, Jiang Wu, Zhihua Zhou, and Zhiming
Wang^{a)}

*State Key Laboratory of Electronic Thin Films and Integrated Devices, University of
Electronic Science and Technology of China, Chengdu 610054, China*

(Received

ABSTRACT

The van der Waals epitaxy of single crystalline Bi₂Se₃ film was achieved on hydrogen passivated Si(111) (H:Si) substrate by physical vapor deposition. Valence band structures of Bi₂Se₃/H:Si heterojunction were investigated by X-ray Photoemission Spectroscopy and Ultraviolet Photoemission Spectroscopy. The measured Schottky barrier height at the Bi₂Se₃-H:Si interface was 0.31 eV. The findings pave the way for economically preparing heterojunctions and multilayers of layered compound families of topological insulators.

PACS: 81.15.Kk, 68.55.-a, 82.80.Pv, 73.30.+y

^{a)}Author to whom correspondence should be addressed: zhmwang@uestc.edu.cn

As a prototype topological insulator (TI), Bi_2Se_3 is characterized with a large bulk band gap (~ 0.3 eV) intercrossed by single-cone-shaped gapless surface states.^{1,2} The single Dirac cone of Bi_2Se_3 is expected to facilitate the exploring of novel quantum phenomenon in TI, and the wide energy band gap will promise a great possibility for room temperature application. Among the efforts in exploring the transport behaviors of Bi_2Se_3 , one featured progress has been made by McIver JW *et al.* that spin-to-momentum conversion (SMC) on the Dirac cone surface states can be detected.³ It also shows that the SMC can be observed in Bi_2Se_3 sample with carrier density as high as $\sim 1 \times 10^{19} \text{ cm}^{-3}$, although a high background doping level of TIs has been thought to hinder access to surface chiral carriers.⁴⁻⁶ However, as an analogue to spin-galvanic effect,⁷ the necessary non-equilibrium spin population to drive the orthogonal-orientated charge current was optically pumped in the experiment of Ref. 3. More recently, a full-electrical SMC scheme was demonstrated by introducing a ferromagnetic metal (FM) spin injector for Bi_2Se_3 TI rather than employing optical orientation procedure used in Ref. 3.⁸ To isolate the stray field of FM electrode from Bi_2Se_3 , a Si spacer layer has to be inserted between FM and TI. Since spin polarized carriers can be effectively injected from the FM electrode and drift quite a long distance through Si without loss of phase coherence,⁹ the SMC efficiency in the proposed device will thus subject to the spin injection efficiency at the Bi_2Se_3 -Si heterointerface.

However, critical information for understanding spin transport behaviors of the Bi_2Se_3 /Si heterojunction such as the relative band positions is still lacking. In this work, thin film growth strategy was employed in order to prepare Bi_2Se_3 /Si junction. X-ray Photoemission Spectroscopy (XPS) and Ultraviolet Photoemission Spectroscopy (UPS)

were conducted to study the core levels (CLs) and valence bands of both thick and thin Bi_2Se_3 films on Si, respectively. We will show that high quality Bi_2Se_3 films can be grown on H-terminated Si(111) (H:Si hereafter) substrates by economical physical vapor deposition (PVD) method. The measured CLs show no chemical shifts between thick (85nm) and thin (10nm) samples further supports the van der Waals epitaxy (vdWE)¹⁰⁻¹³ nature of Bi_2Se_3 on H:Si. Valence band study indicates the Fermi level of as-grown Bi_2Se_3 lies in the conduction band and the calculated Fermi level position is 0.37 eV higher than the Bi_2Se_3 conduction band minimum. Based on XPS and UPS measurements, Shottky barrier height of $\text{Bi}_2\text{Se}_3/\text{H:Si}$ junction is calculated to be 0.31 eV. The band alignment at the $\text{Bi}_2\text{Se}_3/\text{H:Si}$ interface is also pictured.

The growth of the Bi_2Se_3 film was carried out in a home-built PVD facility. A base pressure of 0.5 Pa could be obtained by using a set of rotary pump. High purity (>99.999%) Bi_2Se_3 pellets (Alfa Aesar Inc.) were used as source materials and placed at the hot center of the furnace during the deposition. The resistivity of the Si(111) substrate used in this study was $\sim 100 \Omega\cdot\text{cm}$. H-terminated van der Waals surface of Si(111) was produced by dipping clean Si(111) substrate into diluted HF solution for 10 minute. Prior to the etching process, standard SPM process was employed for cleaning the Si(111) substrates. High purity Argon (>99.999%) was used as feeding gas and the flow rate was held at 0.3 SLM by a mass flow control during the growth process. As soon as the hot center of the furnace was heated to growth temperature (550°C), the Ar flow was supplied which triggered the thin film deposition process. During the growth, the H:Si substrates were in temperature range of 200-250°C and the film thickness could be adjusted by changing growth time. After growth, the films were naturally cooled down to

room temperature then taken out and cut into $5 \times 5 \text{ mm}^2$ samples for further characterizations.

Before performing XPS/UPS studies, structural and surface morphology details of the as-grown films were characterized by X-ray diffraction (XRD) and scanning electron microscopy (SEM), respectively. Using Ecopia HMS-2000 Hall system, carrier concentrations and mobilities of Bi_2Se_3 films were measured. The sample thickness was examined by a Veeco Dekta 150 profilometer. The XPS and UPS measurements (from Omicron GmbH) were carried out *ex situ* in a UHV chamber ($\sim 5 \times 10^{-10}$ mbar) which was equipped with a monochromatized X-ray Al $K\alpha$ source (hv1486.7 eV) for XPS, and a He I source (21.2 eV) for UPS, respectively. The probe area during the XPS and UPS measurements was adjusted to $\sim 1 \text{ mm}^2$ by using the imaging facilities of the system.

The growth of Bi_2Se_3 on H:Si by PVD, in spite of the 7.8% lattice mismatch, exhibited epitaxial nature as confirmed by structural characterizations. Typical XRD θ -2 θ scan of a 110 nm thick Bi_2Se_3 film grown on H:Si substrate was shown in Figure 1 (a). Only the (00n) ($n = 3, 6, 9, 12, \dots$) diffraction peaks of Bi_2Se_3 could be observed indicated the c-axis preferred orientation of the film. In typical XRD Φ scan of Bi_2Se_3 (015) for a thinner Bi_2Se_3 film ($\sim 30 \text{ nm}$), six broad peaks were observed [figure 1(b)] in the scan range of 0° – 360° which depicted in-plane hexagonal ordering of the film. In-plane rotating of Bi_2Se_3 epifilm with respect to the H:Si substrate was negligible as could be seen from the Φ scan peaks of Si(220) [figure 1(c)]. Since rhombohedral crystal lattice of Bi_2Se_3 exhibits three-fold symmetry around the [001] axis, twinning defects were expected to reside in the epifilm. Accordingly, two overlapping epitaxial relationships

characterized respectively as $\text{Bi}_2\text{Se}_3(001)[110]//\text{Si}(111)[112]$ and $\text{Bi}_2\text{Se}_3(001)[110]//\text{Si}(111)[112]$ were inferred to coexist in the epitaxial film.

Figure 2 (a) was an SEM image showing the surface features near a macroscopic scratch on Bi_2Se_3 film. Large size Bi_2Se_3 slabs with smooth surface could be observed. In a magnified SEM image, the growth front features of PVD-grown Bi_2Se_3 film could be clearly illustrated. As could be seen in figure 2 (b), straight bunched steps rather than facets which originated from surface triangular spirals (indicated by dashed triangles) and ran across the whole sample surface were clearly figured out. These surface spiral domains were 180° twinned, which were similar with those morphologies observed in the Bi_2Se_3 films grown by molecular beam epitaxy (MBE) approaches.¹⁴⁻¹⁷ Actually, the unique surface characterizations manifested a spiral growth mode of the PVD-grown film which was also quite identical to the MBE-grown cases. The Bi_2Se_3 film grown by PVD was n-type and highly conductive as measured by van der Pauw Hall with silver paste cured at room temperature used for the contacts. Typical carrier concentration and mobility values were $5 \times 10^{18} \text{ cm}^{-3}$ and $800 \text{ cm}^2\text{V}^{-1}\text{S}^{-1}$, respectively, which were also comparable to that of Bi_2Se_3 films grown on Si by MBE.¹⁴

In the following, XPS and UPS spectrum of Bi_2Se_3 on H:Si were studied. To access the CLs' signals from $\text{Bi}_2\text{Se}_3/\text{H:Si}$ heterointerface, a thick film (110 nm) was firstly thinned by a 3 keV Ar ion sputtering process after it had been loaded into the XPS/UPS analysis chamber. The etch rate of Bi_2Se_3 film during sputtering was $\sim 5 \text{ nm/min}$ as calibrated by another Bi_2Se_3 film sample and the etching was uniform in depth all over the whole sample area as manifested by thickness measurements after sputtering for several minutes. As shown in Figure 3 were the XPS spectrum recorded during the

etching process of a thick Bi_2Se_3 film. No sample charging effect was observed due to the high conductivity of Bi_2Se_3 sample. Curve (a) was from the as-grown surface of the sample, on which C1s and O1s could be clearly seen. After sputtering for 10 min, the two peaks vanished and the rest peaks could be attributed exactly to Bi and Se which indicated a completely removal of contamination on the sample surface as curve (b) shown. The Si $2p$ and $2s$ peaks began to appear at a nominal thickness of 15 nm as indicated in curve (c). As thickness decreasing, the intensity of Si peaks grew rapidly as shown in curve (d)-(f) which indicated that the CLs of both substrate and film were quite accessible at thickness lower than 15 nm. To monitor the surface structure evolution of the Bi_2Se_3 film during the sputtering, low electron energy diffraction (LEED) was employed and no diffraction spots from Si could be observed even as nominal film thickness was down to 4 nm. It indicated unambiguously not only a uniform covering of Bi_2Se_3 thin film on H:Si substrate but also was the thickness uniformity of Bi_2Se_3 grown by PVD method better than $\pm 4\text{nm}$. Both the chemical shifts and the normalized peak intensity proportion of Bi and Se kept constant further depicted the compositional stability of Bi_2Se_3 surface during the Ar ion sputtering process.

After removal of surface contamination, the Bi_2Se_3 film was inspected by UPS and XPS, respectively. Figure 4(a) presented the UPS valence band spectrum from a cleaned Bi_2Se_3 surface (85 nm). In the binding energy range from -2 eV to 6 eV, the UPS curve of the Bi_2Se_3 exhibits two well defined regions. One was at low binding energy where a peak located at around ~ 2.1 eV which could be attributed to Bi $6p$ antibonding.^{18,19} While at $E = 0$ eV, a small peak could be clearly seen which indicated significant electron occupation in the conduction band. Indeed, since the carrier density of Bi_2Se_3 film was

shown to be as high as $\sim 10^{18} \text{ cm}^{-3}$, Fermi level was expected to locate in the conduction band. The VBM of Bi_2Se_3 ($E_{\text{Bi}_{\text{VBM}}}^{\text{Bi}_2\text{Se}_3}$) was determined by the intersection between linear fitting to the leading edge of the spectrum and the background²⁰ and a value of 0.67 eV was obtained. Therefore the Fermi level position in the conduction band was 0.37 eV higher than the conduction band minimum if the band gap of Bi_2Se_3 was taken as 0.3 eV.

The Bi 5*d* core level spectrum of both thick (85nm) and thin (10nm) Bi_2Se_3 film were measured by XPS and shown in Figure 4(b) and (c), respectively. Being a typical heavy metal, spin-orbit splitting in Bi was so large that peaks of 5*d*_{3/2}, 5*d*_{5/2} core levels were clearly separated. However, to precisely determine the peaks' positions, Lorentz–Gauss profiles and Shirley background had been taken for the deconvolution. The binding energies of Bi 5*d*_{5/2} from thick ($E_{\text{Bi}5d_{5/2}}^{\text{Bi}_2\text{Se}_3}$) and thin films ($E_{\text{Bi}5d_{5/2}}^{\text{Bi}_2\text{Se}_3}(i)$) were determined to be 25.27 eV and 25.22 eV respectively. Such a small chemical shift indicated no interfacial reaction occurred between Bi_2Se_3 and H:Si which unambiguously evidenced the vdWE nature of Bi_2Se_3 grown on H:Si.

The Si 2*p* CLs from the thin Bi_2Se_3 film (10nm) covered H:Si were also studied. For the Si 2*p* spectrum, curve fitting schemes were employed to distinguish the precise positions of overlapped 2*p*_{3/2} and 2*p*_{1/2} peaks. The curves were constrained by documented spin-orbit splitting,²¹ intensity ratio, and FWHM ratio of H:Si peak given in this work. The best fit based on the given constraints was shown in figure 4(d) and Si 2*p*_{3/2} position, $E_{\text{Si}2p_{3/2}}^{\text{H:Si}}(i)$ was 99.70 eV.

Using the values of CLs and VBM obtained in XPS and UPS measurements, the valence band offset (VBO) can thus be calculated by using the Kraut equation:²²

$$E_{\text{VBO}} = E_{\text{CL}} + (E_{\text{Si}2p_{3/2}}^{\text{H:Si}} - E_{\text{SiVBM}}^{\text{H:Si}}) - (E_{\text{Bi}5d_{5/2}}^{\text{Bi}_2\text{Se}_3} - E_{\text{BiVBM}}^{\text{Bi}_2\text{Se}_3}), \quad (1)$$

and the Schottky barrier height Φ_{B} is given by

$$\Phi_{\text{B}} = (E_{\text{Si}2p_{3/2}}^{\text{H:Si}} - E_{\text{SiVBM}}^{\text{H:Si}}) + E_{\text{G}}^{\text{H:Si}} - E_{\text{Si}2p_{3/2}}^{\text{H:Si}}(i), \quad (2)$$

Where $E_{\text{CL}} = E_{\text{Bi}5d_{5/2}}^{\text{Bi}_2\text{Se}_3}(i) - E_{\text{Si}2p_{3/2}}^{\text{H:Si}}(i)$ is the CL offset at the interface. $E_{\text{G}}^{\text{H:Si}}$, $E_{\text{Si}2p_{3/2}}^{\text{H:Si}}$, and $E_{\text{SiVBM}}^{\text{H:Si}}$ are values of band gap, CL energy, and VBM from bulk H:Si, respectively.

From Eq. (1), the E_{VBO} , can be calculated with measured values of $(E_{\text{Bi}5d_{5/2}}^{\text{Bi}_2\text{Se}_3} - E_{\text{BiVBM}}^{\text{Bi}_2\text{Se}_3})$, E_{CL} , and documented value of $(E_{\text{Si}2p_{3/2}}^{\text{H:Si}} - E_{\text{SiVBM}}^{\text{H:Si}})^{23}$, and is 0.19 eV. From Eq. (2), Schottky barrier height Φ_{B} can be calculated with measured value of $E_{\text{Si}2p_{3/2}}^{\text{H:Si}}(i)$ and documented values of $E_{\text{G}}^{\text{H:Si}}$ and $(E_{\text{Si}2p_{3/2}}^{\text{H:Si}} - E_{\text{SiVBM}}^{\text{H:Si}})$, and is 0.31 eV. Compared with the electronically measured Schottky barrier (0.34 eV),⁸ the XPS/UPS measured value in our work is smaller. This may be due to the silicon substrates employed in our experiment have higher resistivity (i.e., higher electron affinity). Moreover, the sharp interface between the epitaxial Bi_2Se_3 layer and H:Si surface will contribute to eliminating interfacial potential fluctuations thus an ideal Schottky junction structure is expected. Finally, the band diagram of $\text{Bi}_2\text{Se}_3/\text{H:Si}$ heterojunction is schematically indicated in figure 5.

In summary, we successfully prepared single crystalline Bi_2Se_3 films on H-terminated Si(111) surface by PVD method. Based on precise XPS and UPS measurements, the Schottky barrier and band alignment of $\text{Bi}_2\text{Se}_3/\text{H:Si}$ heterostructure were calculated and illustrated, respectively. The vdWE scheme, which had only been considered responsible for MBE growth of layered compounds on chemically inert substrates with large lattice mismatch, was proved valid for the more economical PVD

method. Another advantage of growing Bi_2Se_3 on H:Si van der Waals surface is that the TI Dirac cone of Bi_2Se_3 at the interface can be effectively preserved. Indeed, very small chemical shifts (0.05 eV) of Bi $5d$ CLs between bulk Bi_2Se_3 and $\text{Bi}_2\text{Se}_3/\text{H:Si}$ interface was experimentally confirmed in this work which reflected the weak bonding nature between Bi_2Se_3 epilayers and H:Si substrates. Considering the layered compound families of TIs share similar crystal structure of Bi_2Se_3 , our findings may serve as useful reference for preparing heterostructures and multilayers of them in an economical way.

ACKNOWLEDGEMENTS

This work is supported by the National Natural Science Foundation of China under Grant No. 11104010 and the Fundamental Research Funds for the Central Universities of China under Grant No. ZYGX2012J033.

REFERENCES

- ¹ D. Hsieh, Y. Xia, D. Qian, L. Wray, J. H. Dil, F. Meier, J. Osterwalder, L. Patthey, J. G. Checkelsky, N. P. Ong, A. V. Fedorov, H. Lin, A. Bansil, D. Grauer, Y. S. Hor, R. J. Cava, and M. Z. Hasan, *Nature* **460**, 1101 (2009).
- ² H. J. Zhang, C. X. Liu, X. L. Qi, X. Dai, Z. Fang, and S. C. Zhang, *Nat. Phys.* **5**, 438 (2009).
- ³ J. W. McIver, D. Hsieh, H. Steinberg, P. Jarillo-Herrero, and N. Gedik, *Nat. Nanotechnol.* **7**, 96 (2012).
- ⁴ J. G. Analytis, J. H. Chu, Y. L. Chen, F. Corredor, R. D. McDonald, Z. X. Shen, and I. R. Fisher, *Phys. Rev. B* **81**, 205407 (2010).
- ⁵ N. P. Butch, K. Kirshenbaum, P. Syers, A. B. Sushkov, G. S. Jenkins, H. D. Drew, and J. Paglione, *Phys. Rev. B* **81**, 241301 (2010).
- ⁶ T. Arakane, T. Sato, S. Souma, K. Kosaka, K. Nakayama, M. Komatsu, T. Takahashi, Z. Ren, K. Segawa, and Y. Ando, *Nat. Commun.* **3**, 636 (2012).
- ⁷ S. D. Ganichev, E. L. Ivchenko, V. V. Bel'kov, S. A. Tarasenko, M. Sollinger, D. Weiss, W. Wegscheider, and W. Prettl, *Nature* **417**, 153 (2002).
- ⁸ C. Ojeda-Aristizabal, M. S. Fuhrer, N. P. Butch, J. Paglione, and I. Appelbaum, *Appl. Phys. Lett.* **101**, 023102 (2012).
- ⁹ I. Appelbaum, B. Huang, and D. J. Monsma, *Nature* **447**, 295 (2007).
- ¹⁰ A. Koma, K. Sunouchi, and T. Miyajima, *J. Vac. Sci. Technol. B* **3**, 724 (1985).
- ¹¹ A. Koma and K. Yoshimura, *Surf. Sci.* **174**, 556 (1986).
- ¹² A. Koma, *Thin Solid Films* **216**, 72 (1992).
- ¹³ A. Koma, *Surf. Sci.* **267**, 29 (1992).

- ¹⁴ H. D. Li, Z. Y. Wang, X. Kan, X. Guo, H. T. He, Z. Wang, J. N. Wang, T. L. Wong, N. Wang, and M. H. Xie, *New J. Phys.* **12**, 103038 (2010).
- ¹⁵ H. D. Li, Z. Y. Wang, X. Guo, T. L. Wong, N. Wang, and M. H. Xie, *Appl. Phys. Lett.* **98**, 043104 (2011).
- ¹⁶ X. Chen, X. C. Ma, K. He, J. F. Jia, and Q. K. Xue, *Adv. Mater.* **23**, 1162 (2011).
- ¹⁷ N. V. Tarakina, S. Schreyeck, T. Borzenko, C. Schumacher, G. Karczewski, K. Brunner, C. Gould, H. Buhmann, and L. W. Molenkamp, *Cryst. Growth Des.* **12**, 1913 (2012).
- ¹⁸ Y. Ueda, A. Furuta, H. Okuda, M. Nakatake, H. Sato, H. Namatame, and M. Taniguchi, *J. Electron Spec. Rel. Phen.* **101**, 677 (1999).
- ¹⁹ V. B. Nascimento, V. E. de Carvalho, R. Paniago, E. A. Soares, L. O. Ladeira, and H. D. Pfannes, *J. Electron Spec. Rel. Phen.* **104**, 99 (1999).
- ²⁰ S. A. Chambers, T. Droubay, T. C. Kaspar, and M. Gutowski, *J. Vac. Sci. Technol. B* **22**, 2205 (2004).
- ²¹ T. Gleim, L. Weinhardt, T. Schmidt, R. Fink, C. Heske, E. Umbach, L. Hansen, G. Landwehr, A. Waag, A. Fleszar, B. Richter, C. Ammon, M. Probst, and H. P. Steinruck, *Phys. Rev. B* **67**, 205315 (2003).
- ²² E. A. Kraut, R. W. Grant, J. R. Waldrop, and S. P. Kowalczyk, *Phys. Rev. Lett.* **44**, 1620 (1980).
- ²³ L. J. Webb, E. J. Nemanick, J. S. Biteen, D. W. Knapp, D. J. Michalak, M. C. Traub, A. S. Y. Chan, B. S. Brunschwig, and N. S. Lewis, *J. Phys. Chem. B* **109**, 3930 (2005).

FIGURE LEGENDS

FIG. 1. (a) XRD out-of-plane θ - 2θ scan of a 110 nm thick Bi_2Se_3 thin film grown on H:Si substrate. The in-plane Φ scans of Bi_2Se_3 (015) and of Si (220) from the same sample were shown in (b) and (c), respectively. The thickness of the film used in XRD Φ scans was 30 nm.

FIG. 2. (a) Large-scale SEM image shows the surface morphology near a scratch on a 110 nm thick Bi_2Se_3 film. (b) A magnified SEM image taken on the same sample illustrates the step bunching features of Bi_2Se_3 surface. The dashed triangles pointed left and right respectively indicate the existence of rotation domain pairs.

FIG. 3. (Color online) XPS measurements on Bi_2Se_3 film on H:Si(111) before (a) and after Ar ion sputtering (b)-(e). The nominal film thickness of Bi_2Se_3 in (b) to (e) is 85 nm, 15 nm, 10 nm, 6 nm, and 4 nm, respectively. Inset is a typical LEED image ($E = 75$ eV) taken from 10 nm Bi_2Se_3 film during the sputtering.

FIG. 4. (Color online) (a) Valence band maximum measured by UPS and (b) Core level energy spectrum measured by XPS for cleaned Bi_2Se_3 film with nominal thickness of 85nm. Core level energy spectrum measured by XPS for Bi_2Se_3 film with nominal thickness of 10 nm on H:Si(111) are shown in (c) and (d). Dotted curves are original data.

FIG. 5. (Color online) The schematic band diagram for Bi_2Se_3 on H:Si(111) heterojunction system. $E_C^{\text{Bi}_2\text{Se}_3}$ and $E_C^{\text{H:Si}}$ represent conduction band minima of Bi_2Se_3 and H:Si, respectively.

FIGURES

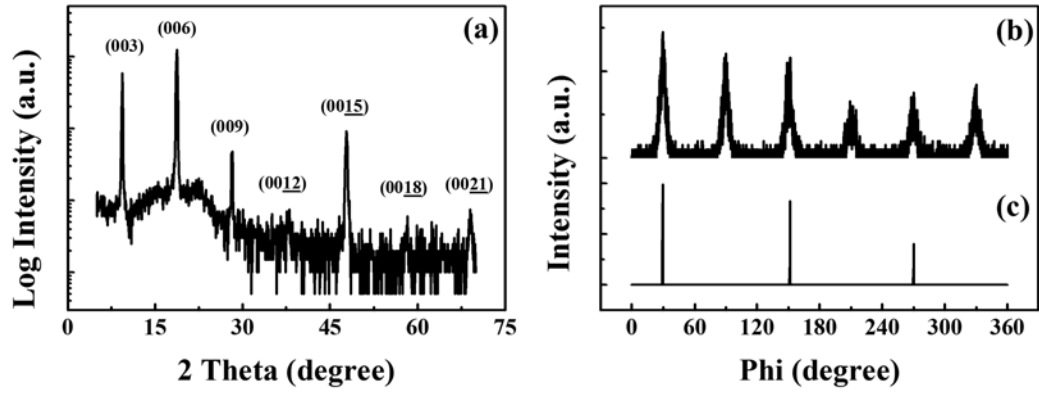


FIG. 1.

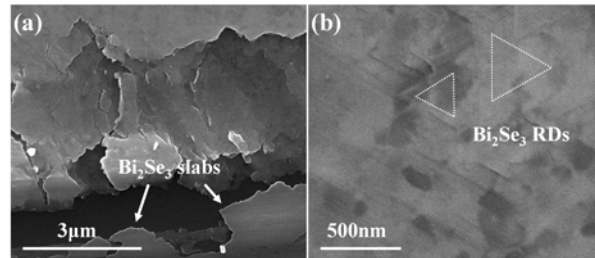


FIG. 2.

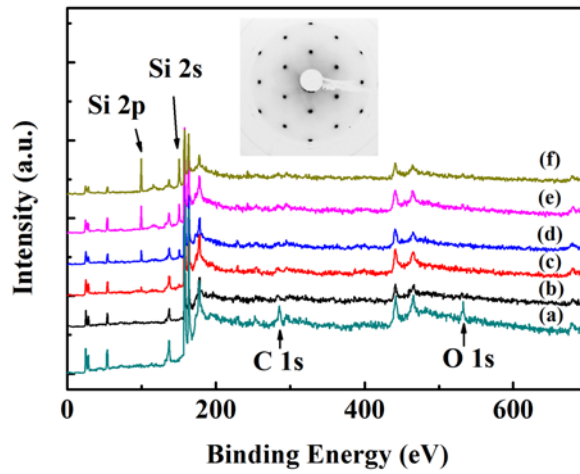


FIG. 3.

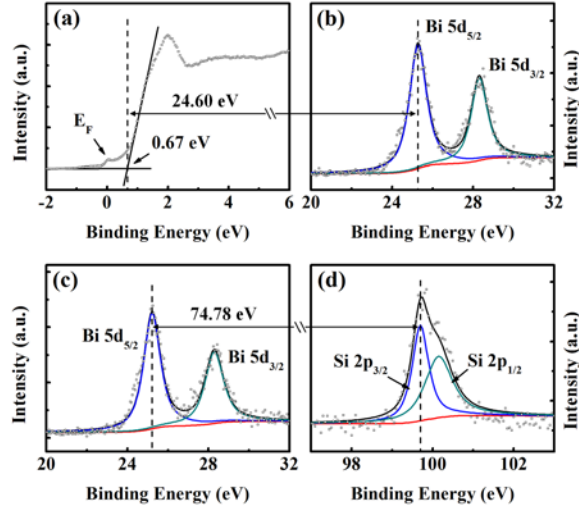


FIG. 4.

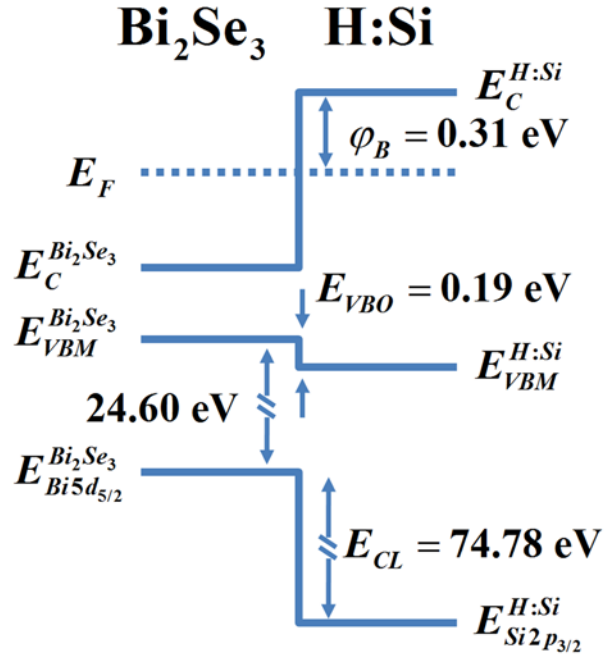


FIG. 5.